SUPPORTING INFORMATION

Supporting Information

Palladium Recovery from Acidic Solution with Phenanthroline-Based Covalent Organic Polymers as Adsorbents for Efficient Heterogeneous Catalysis

Hui Liu,[a] Pengcheng Wu,[a] Ke Wang,[a] Qing Li,[b] Chengkan Yu,[a] Xiaowei Li,[a] Yimin Cai,*[a] Wen Feng*[a] and Lihua Yuan*[a]

[a.] College of Chemistry, Key Laboratory of Radiation Physics and Technology of the Ministry of Education, Institute of Nuclear Science and Technology, Sichuan University, Chengdu 610064, China.

[b.] Biotechnology and Nuclear Technology Research Institute, Sichuan Academy of Agricultural Sciences, Chengdu 610061, China.

SUPPORTING INFORMATION

Contents

SUPPORTING INFORMATION

1. Materials and Methods

Chemicals and reagents. All metal ions ($Pd(NO_3)_2 \cdot 2H_2O$, $Ni(NO_3)_2 \cdot 6H_2O$, $La(NO_3)_3 \cdot 6H_2O$, $Cd(NO_3)_2 \cdot 4H_2O$, $Eu(NO_3)_3 \cdot 6H_2O$, $Yb(NO_3)_3$, $Sm(NO_3)_3$, $Pr(NO_3)_3$, $Ba(NO_3)_2$, $Sr(NO_3)_2$, $Fe(NO_3)_3 \cdot 9H_2O$, $Nd(NO_3)_3$, $RbNO_3$, $CsNO_3$, $AgNO_3$, $KReO_4$, $Na_2MoO_4 \cdot 2H_2O$, and $NaNO_3$, 99.9%) used in adsorption experiments were obtained from Aladdin Industrial Corporation, Adamas Reagent, Ltd., and Energy Chemical Co. Ltd. as their purest forms. 4-aminobenzonitrile (98%), trifluoromethanesulfonic acid (99%), 2,9-dimethyl-1,10-phenanthroline (98%), selenium dioxide (98%), and the other reagents and solvents were purchased from Energy Chemical Co. Ltd. in analytical pure (AR) and used without further purification.

Characterization. The ^1H NMR spectra of TAPT and Phen-CHO were obtained from a Bruker AVANCE III HD-400 MHZ. Solid-state cross-polarization magic angle spinning (CP/MAS) ^{13}C NMR experiments were performed with a Bruker AVANCE III 500MHz and Fourier transform infrared (FT-IR) spectroscopy in the range of 400-4000 cm^{-1} was investigated by a Bruker ALPHA infrared spectrometer. The thermostability of COPs was tested by using DTG-60 (H) at a rate of 10 ^oC/min under a nitrogen atmosphere. The element contents of C, H, O, N, and Pd were measured with an organic element analyzer (Flash EA 1112). Powder X-ray diffraction (PXRD) patterns were recorded on Schimadzu-XRD6100 and DX-2700 diffractometer. Scanning electron microscopy (SEM) and energy-dispersive X-ray spectroscopy (EDS) data were collected on a ZEISS Gemini 300 microscope. The nitrogen adsorption isotherms were determined on an Automated Gas Adsorption Analyzer (Autosorb-IQ) at 77 K, and the samples were degassed under vacuum at 120 °C for 12 h before the test. X-ray photoelectron spectroscopy (XPS) was studied with a Shimadzu/Krayos AXIS Ultra DLD. Elemental analysis experiment was performed on an organic element analyzer (Flash EA 1112). The concentrations of metal ions in the aqueous phase were determined by an Inductively Coupled Plasma-Optical Emission Spectrometer (ICP-OES, PerkinElmer ICP optima 8000).

Pd(II) adsorption experiments. Pd(II) solutions with different concentrations of 25-818 mg L^{-1} were prepared by dissolving $Pd(NO_3)_2(H_2O)_2$ in 1-6 M HNO_3. All experiments were conducted at 25 °C with a solid/liquid ratio of 0.5 g/L except for adsorption thermodynamics tests and recyclability investigations of COPs. In a general procedure, COP-1/COP-2 (5 mg) was added into an aqueous solution containing a certain content of Pd(II) (10 mL), and the mixture was shaken at 298 K for the required time. After filtration with a 0.22 μm nylon

membrane filter, the concentrations of Pd(II) and other metal ions in aqueous solution were measured by ICP-OES. All the sorption experiments were carried out at least twice with acceptable errors.

Influence of nitric acid concentration. The effect of acidity on Pd^{2+} sorption was studied by varying the concentration of nitric acid from 1 to 6 M. COP-1/COP-2 (5 mg) was mixed with 10 mL Pd(II) solution (102-105 mg L^{-1}). After 15 h, the obtained mixture was filtered before ICP-OES analysis.

Adsorption isotherms. The sorption isotherm experiments were carried out with various initial Pd^{2+} concentrations ranging from 25 to 818 ppm. In each sample, COP-1/COP-2 (5 mg) was added into Pd^{2+} solution (10 mL) in 3 M nitric acid. After being shaken for 15 h, the aqueous phase was separated for ICP-OES analysis. The amount of adsorbed palladium (q_e, mg g^{-1}) was calculated using equation (1), and the adsorption isotherm data were then fitted with Langmuir isotherm model (2) and Freundlich isotherm model (3).[1, 2]

$$q_e = \frac{(C_0 - C_e)V}{m} \quad (1)$$

$$\frac{C_e}{q_e} = \frac{1}{b_1 q_m} + \frac{C_e}{q_m} \quad (2)$$

$$\ln q_e = \ln K_F + \frac{1}{n} \ln c_e \quad (3)$$

where C_0 (mg L^{-1}) and C_e (mg g^{-1}) are the initial and equilibrium concentrations of Pd^{2+}, respectively. V is the volume of the solution and m is the weight of COPs. q_m (mg g^{-1}) stands for the maximum adsorption capacity, and b_1 denotes a constant revealing the affinity between the sorbate and adsorbent. K_F ($mg^{1-1/n}$ $L^{1/n}$ g^{-1}) is a constant value related to the sorption capacity and n refers to an indicator related to the heterogeneity of the surface of the adsorbent.

Adsorption kinetics. The experiments were performed in 3 M nitric acid with a solid/liquid ratio of 0.5 g/L. As soon as COP-1/COP-2 (50 mg) was added into Pd(II) solution (100 mL, 99 ppm), an aliquot (0.2 mL) was collected at various contact times for analysis of the residual palladium concentration. The experimental data were fitted with the kinetics models of pseudo-first-order (4), pseudo-second-order (5), and intraparticle diffusion (6).[3]

$$\ln(q_e - q_t) = \ln q_e - k_1 t \quad (4)$$

$$\frac{t}{q_t} = \frac{1}{k_2 q_e^2} + \frac{t}{q_e} \quad (5)$$

$$q_t = k_{int} t^{0.5} + C \quad (6)$$

where q_e (mg g^{-1}) and q_t (mg g^{-1}) correspond to the adsorption amounts at equilibrium and at specific contact times t, respectively. k_1 (h^{-1}) and k_2 (g mg^{-1} h^{-1}) are the rate constants. In the

intraparticle diffusion model, k_{int} (mg g^{-1} $h^{-0.5}$) is the intraparticle diffusion rate constant, and C (mg g^{-1}) is a constant related to the thickness of the boundary layer.

Adsorption thermodynamics. The mixture of COP-1/COP-2 (5 mg) and Pd(II) solution (10 mL, 98 ppm) was stirred for 5 h at a different temperature varying from 285 K to 315 K. Then the residual Pd^{2+} in the aqueous phase was measured by ICP-OES. The data were fitted with equation (7) and equation (8) to obtain thermodynamic parameters (ΔH, ΔS, ΔG).

$$\ln K_d = \frac{\Delta S}{R} - \frac{\Delta H}{RT} \quad (7)$$

$$\Delta G = \Delta H - T\Delta S \quad (8)$$

where K_d is the distribution coefficient, R is the ideal gas constant (8.314 J mol^{-1} K^{-1}), T is the absolute temperature (K), ΔH, ΔS, and ΔG are enthalpy change (kJ mol^{-1}), entropy change (J mo^{-1} K^{-1}), and Gibbs free energy change (kJ mol^{-1}), respectively.

Selective adsorption for palladium. The selectivity of COPs for Pd(II) was studied using simulated high-level liquid waste (HLLW) with a solid/liquid ratio of 0.5 g L^{-1}. The simulated HLLW was prepared by dissolving 18 metal salts in 3 M HNO_3, which were listed in Table S5. COP-1/COP-2 (5 mg) was added into simulated HLLW (10 mL), then the mixture was stirred for 15 h. After filtration, the filtrate was analyzed with ICP-OES to determine the residual metal concentration. The distribution coefficient (K_d, mL/g) and separation factor ($SF_{Pd/M}$) were calculated using the following equation (9) and (10), respectively.

$$K_d = \frac{C_0 - C_e}{C_e} \times \frac{V}{m} \quad (9)$$

$$S_F = \frac{K_{d(Pd)}}{K_{d(M)}} \quad (10)$$

where C_0 (mg L^{-1}) and C_e (mg g^{-1}) are the initial and equilibrium concentrations of Pd^{2+}, respectively. V (mL) is volume of the solution and m (g) is the weight of COPs.

Desorption and recyclability. COP-1/COP-2 (50 mg) was first shaken with a Pd^{2+} solution (100 mL, 107 ppm) for 12 h. Subsequently, COP-1-Pd or COP-2-Pd was eluted by the 0.5 M thiourea/1 M HCl solution (12 h, 100 mL) and water (12 h, 100 mL × 3) in sequence. The regenerated adsorbents were collected and used for the next sorption/desorption cycle.

Dynamic column adsorption experiments. Degreasing cotton and silica gel were firstly filled in the column to prevent the loss of adsorbent. Then, a mixture of COP-2 (100 mg) and silica gel was packed into the column. After that, a Pd^{2+} solution (50 ppm) in 3 M HNO_3 went through the column at a flow rate of 0.8 mL/min at room temperature. After the column reached adsorption saturation, deionized water was used to remove the residual palladium in the pipeline. Then 0.5 M thiourea solution in 1 M HCl was used to elute the adsorbed Pd(II) ions. Finally,

the concentration of the Pd(II) in eluents was analyzed by ICP-OES, and the adsorbed amount (q'_e, mg/g) and desorption efficiency (*Des*, %) were calculated by the following equations:

$$q'_e = \frac{(C_0 - C_{V_1})V_1}{m} \quad (11)$$

$$Des\% = \frac{q'_e - \frac{C_d V_2}{m}}{q'_e} \times 100\% \quad (12)$$

where C_0 (mg L^{-1}) and C_{V1} (mg L^{-1}) are initial and effluent concentration of Pd^{2+}, C_d (ppm) is Pd^{2+} concentration in desorption eluent, while m (g), V_1 (L) and V_2 (L) are the mass of adsorbent, the volume of effluent and the volume of desorption solution, respectively.

Radiation resistance tests. The radiation tests were conducted by a ^{60}Co gamma source at a dose rate of 7.63 kGy h^{-1}. COP-1/COP-2 (50 mg) was exposed to the γ-irradiation for five doses (200, 300, 400, 500, and 600 kGy). Then, the FT-IR spectra of the irradiated samples were measured. Meanwhile, the mixture of irradiated materials (5 mg) and a Pd(II) solution (10 mL, 101 ppm) was stirred for 15 h. After filtration, the concentration of residual Pd(II) was determined by ICP-OES.

Density functional theory (DFT) calculation. DFT calculations were carried out using the Gaussian 09 program to analyze the interaction between the repeating unit as a fragment of COPs and $Pd(NO_3)_2$. **L₁** and **L₂** were used as models for mimicking the local structures of the amorphous sorbent materials of COP-1 and COP-2. The B3LYP-D3/SDD~6-31G* was employed to optimize the geometries of the model structures and the palladium complexes in water.[4] For these optimized structures, higher precision single-point energy calculations were performed at the M06-2×-D3/SDD~6-311++G** level, and the SMD model was utilized to consider the solvent effect. The binding energies were calculated according to the following equation:

$$E_b = E_{product} - E_{rectant} \quad (13)$$

$$E_b = E_{complex} - E_{ligand} - E_{Pd(NO_3)_2\,(H_2O)_2} - n\,E_{H_2O} \cdots \text{n = 1, 2} \quad (14)$$

where the $E_{complex}$, E_{ligand}, E_{Pd} and E_{H_2O} indicate the total energies of each complex, **L₁** and **L₂**, $Pd(NO_3)_2(H_2O)_2$ and H_2O, respectively.

General procedure for Suzuki-Miyaura cross-coupling reaction. COP-2 (250 mg) was immersed in a Pd(II) solution (100 ml, 748 ppm) at 3 M HNO_3, followed by washing with water and drying to afford an orange powder containing 14% Pd(II) in mass. COP-2-Pd(II) was reduced by $NaBH_4$ to give COP-2-Pd(0) containing 16% Pd(II) in mass. A mixture of catalyst (1mol% Pd), aryl halide (1.0 mmol), boronic acid (1.5 mmol), K_2CO_3 (2.0 mmol) in H_2O (5

mL) was stirred at 100°C for the required time under nitrogen. After completion of the reaction, the mixture was cooled down to room temperature and extracted with ethyl acetate (10 mL). Then, the organic phase was separated. After dried with anhydrous Na_2SO_4, the solvent was removed under reduced pressure to get the crude product, while the catalyst remained in the aqueous phase was filtered to recover for reuse.

2. Synthesis

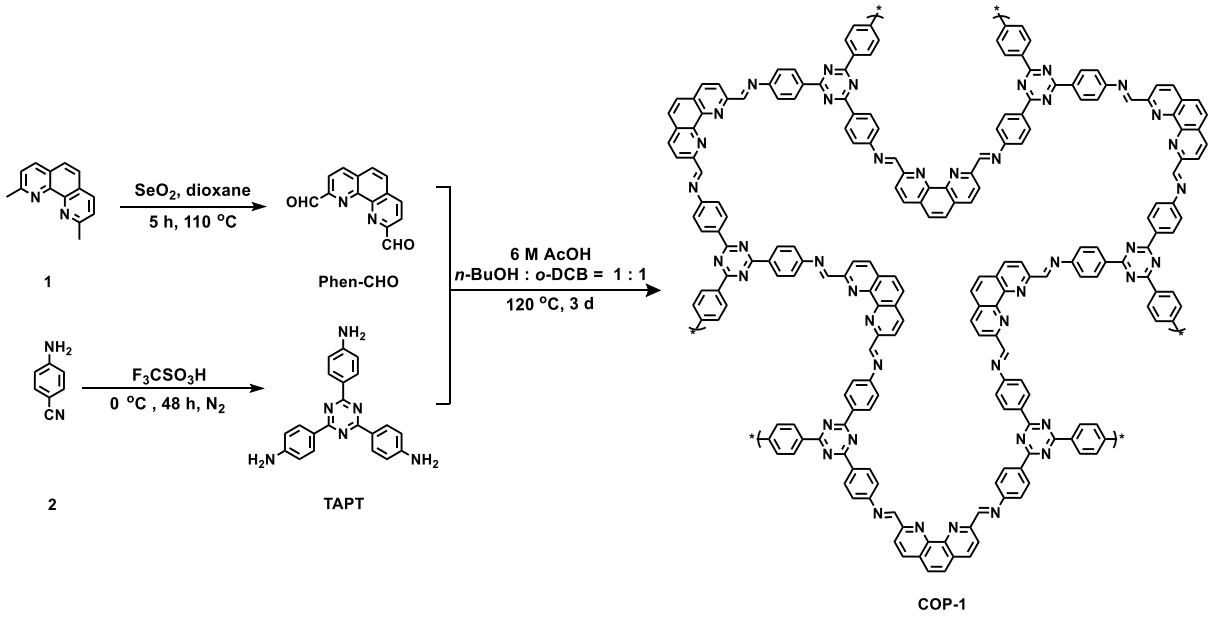

Scheme S1. Synthetic routes of COP-1.

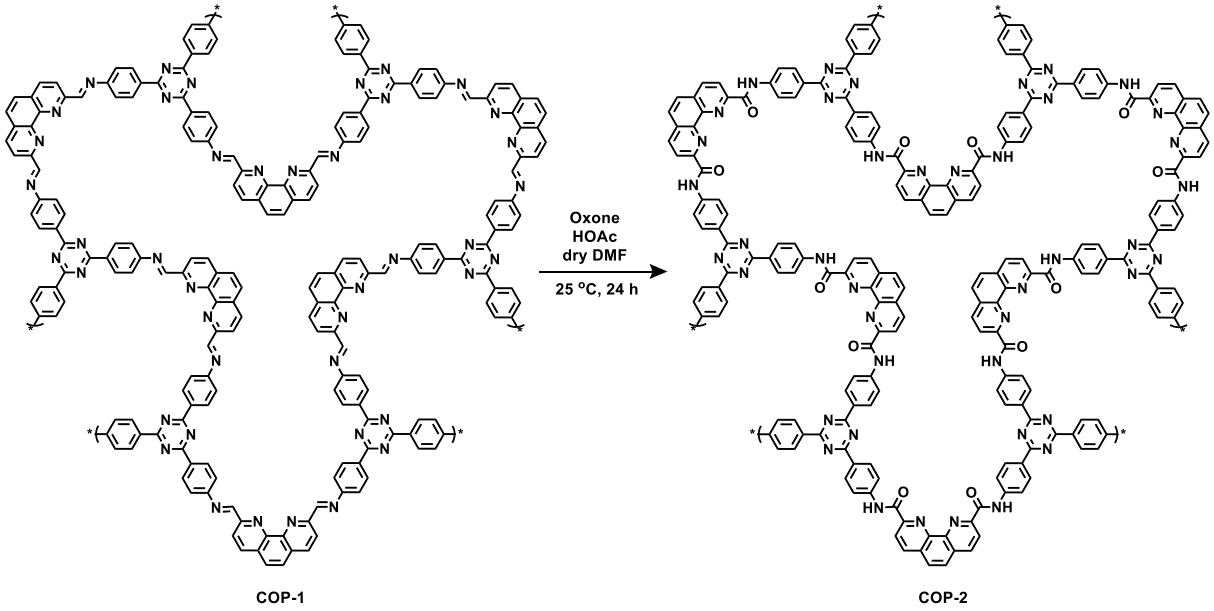

Scheme S2. Synthetic route of COP-2.

Synthesis of 1,10-Phenanthroline-2,9-dicarbaldehyde (Phen-CHO).[5] Selenium dioxide (8.00 g, 72.0 mmol) was dissolved in 1,4-dioxane (150 mL) and water (8 mL). Then the mixture

was stirred and heated to reflux in a 500 mL round bottom flask. A solution of 2,9-dimethyl-1,10-phenanthroline (5.00 g, 24.0 mmol) in 1,4-dioxane (100 mL) was added to the flask over 30 min and refluxed for 6 h, after which the hot reaction mixture was filtered through a bed of celite. Yellow crystals precipitated from the filtrate upon cooling to 0 °C. The resulting crude product was collected and purified by column chromatography using the silica gel (DCM/MeOH, 10/1, v/v) to give a yellow solid, 2.30 g (Yield: 41%). ^{1}H NMR (400 MHz, $CDCl_3$) δ 10.36 (s, 2H), 8.80 (d, J = 8.4 Hz, 2H), 8.31 (d, J = 8.4 Hz, 2H), 8.29 (s, 2H).

Synthesis of 1,3,5-tris-(4-aminophenyl) triazine (TAPT). [6] 4-Aminobenzonitrile (2.00 g, 16.9 mmol) was taken in a 50 mL two-necked round bottom flask placed in ice-water. Then trifluoromethanesulfonic acid (5.1 mL, 57.5 mmol) was added dropwise for 30 min in an inert atmosphere. Next, the mixture was stirred for 48 h at room temperature. After the completion of the reaction, deionized water (40 mL) water was added to the mixture and it was neutralized by adding 2M NaOH solution until the pH reaches to 7. Finally, the precipitate was collected and washed with water (50 mL × 3), then dried under vacuum to give a yellow product, 1.41 g (Yield: 70%). ^{1}H NMR (400 MHz, DMSO-d_6) δ 8.34 (d, J = 8.4 Hz, 6H), 6.69 (d, J = 8.4 Hz, 6H), 5.90 (s, 6H).

Synthesis of COP-1. In an inert atmosphere, TAPT (1.00 g, 2.8 mmol), Phen-CHO (1.00 g, 4.2 mmol), 1-butanol (20 mL), *o*-dichlorobenzene (20 mL), and 6 M aqueous acetic acid solution (10 mL) were added into a round bottom flask. The reaction mixture was heated at 120 °C for 72 h, then it was allowed to cool to room temperature. A dark brown powder was collected by centrifugation, washed with DMF (12 h, 50 mL × 3), and then subjected to Soxhlet extraction with THF for 48 h. After drying under vacuum at 60 °C for 12 h, COP-1 was obtained as dark red powder, 1.62 g (yield: 85%).

Synthesis of COP-2. The mixture of COP-1 (450 mg), dry Oxone (1.86 g, 3.0 mmol), and acetic acid (0.90 mL) in dry DMF (17 mL) was stirred under an inert atmosphere at 25 °C for 24 hours. Then the solid was collected by filtration, and washed with aqueous $Na_2S_2O_3$ solution (10%), water, and THF, successively. After being subjected to Soxhlet extraction with THF for 48 h and dried under vacuum at 60 °C for 12 h, the product was obtained as a brown solid, 0.42 g (yield: 86%).

3. Characterization of Materials

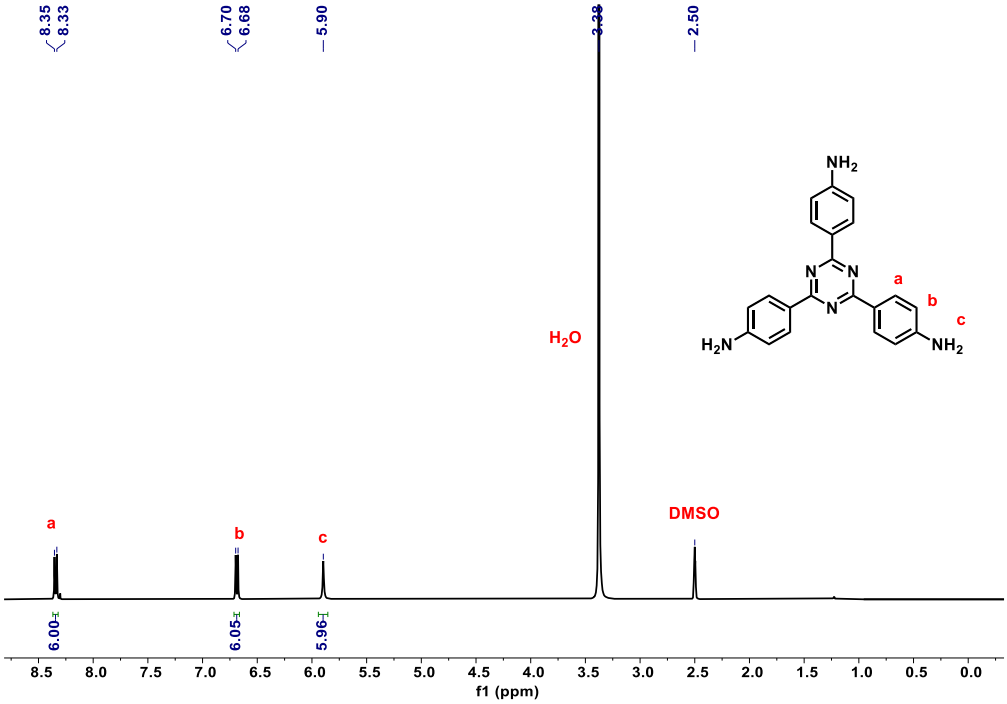

Fig. S1 ^{1}H NMR spectrum (400 MHz, DMSO-d_6, 298 K) of TAPT.

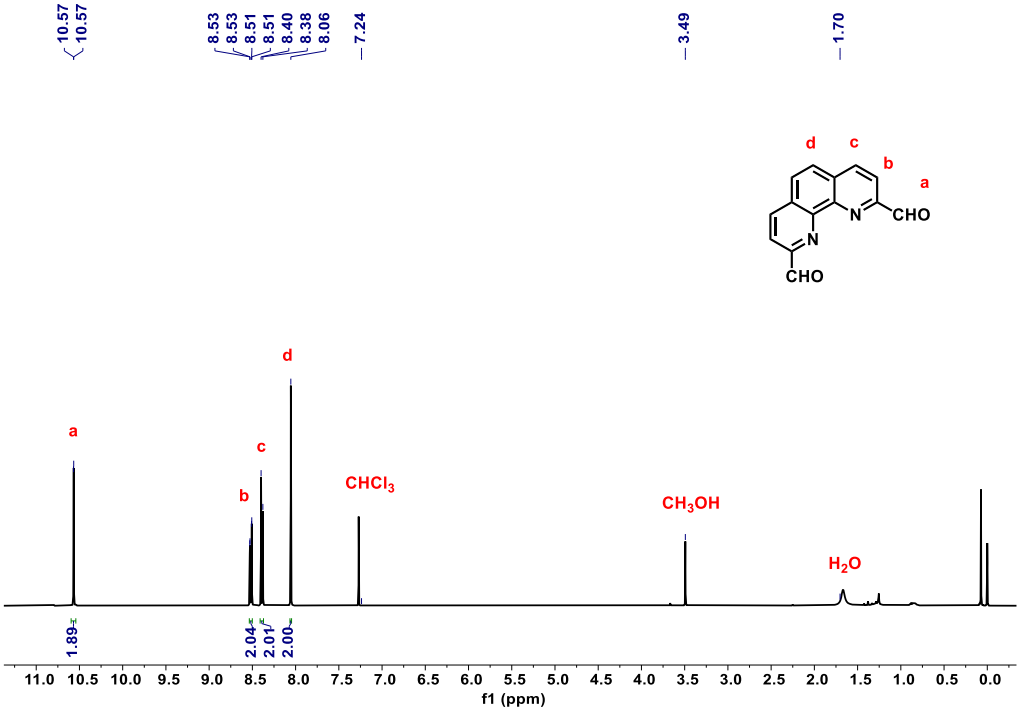

Fig. S2 ^{1}H NMR spectrum (400 MHz, $CDCl_3$, 298 K) of Phen-CHO.

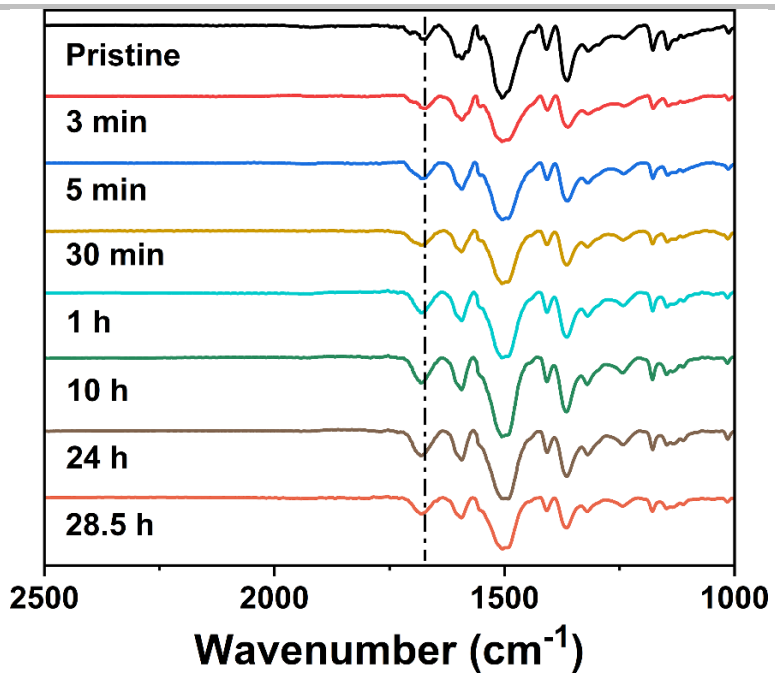

Fig. S3 FT-IR spectra of COP-1 at different oxidation times.

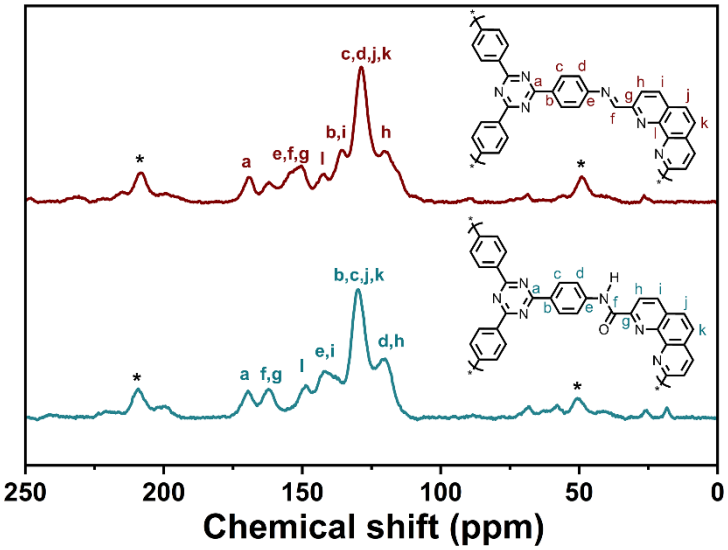

Fig. S4 Solid-state CP-MAS ^{13}C NMR spectra of COP-1 (top) and COP-2 (bottom) (spinning rate 8 kHz). Asterisks denote spinning sidebands.

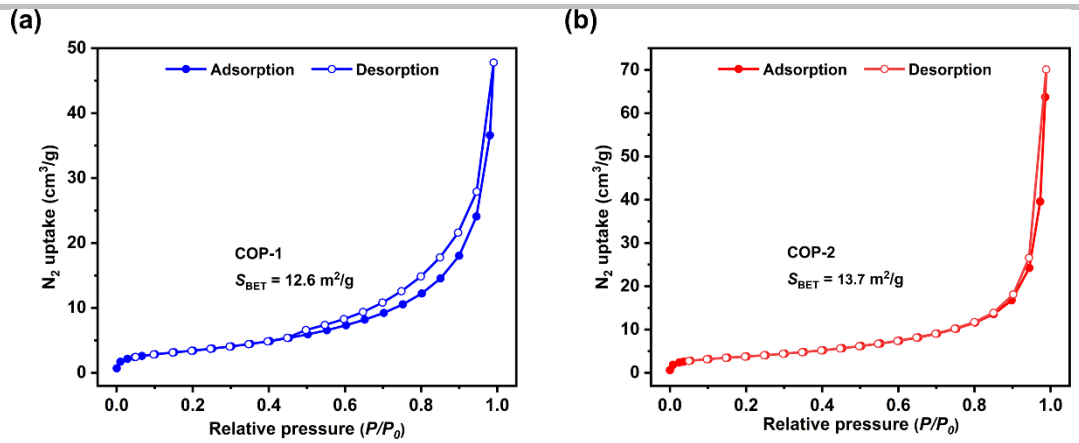

Fig. S5 N_2 adsorption isotherms at 77 K for (a) COP-1 and (b) COP-2.

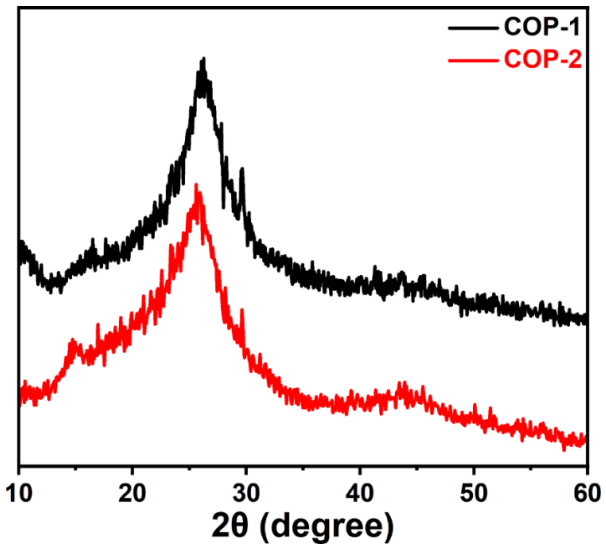

Fig. S6 PXRD data of COP-1 and COP-2.

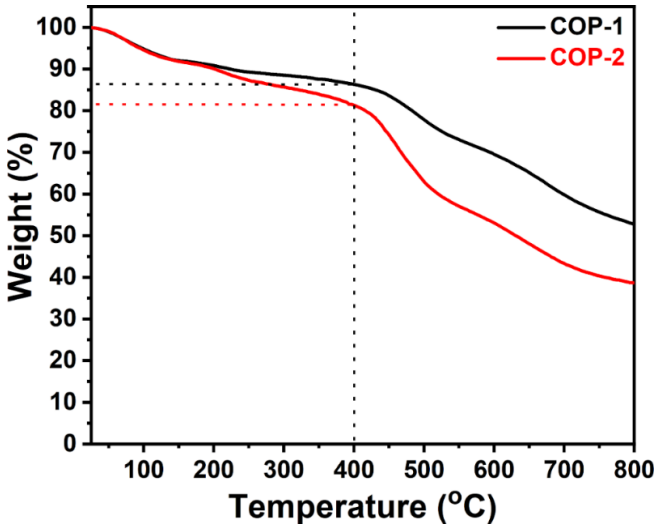

Fig. S7 TGA curves for COP-1 and COP-2.

4. Adsorption Experiments

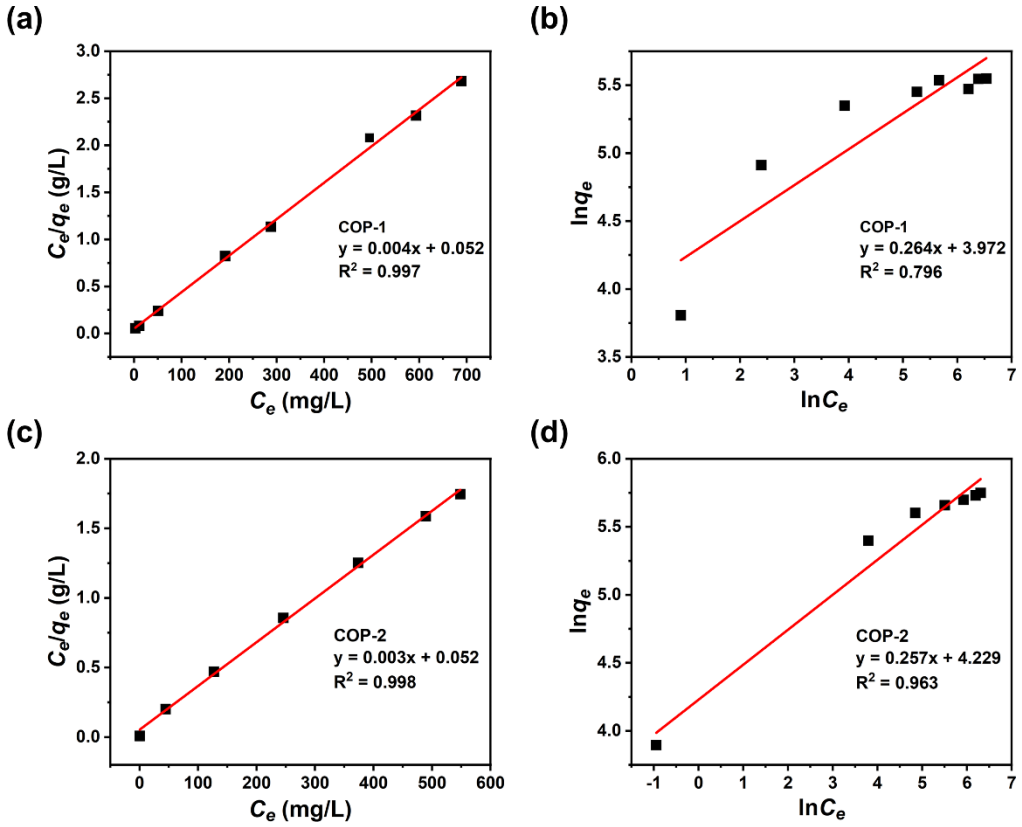

Fig. S8 (a) Langmuir and (b) Freundlich model plots for palladium adsorption onto COP-1, (c) Langmuir and (d) Freundlich model plots for palladium adsorption onto COP-2.

Table S1 Isotherm parameters for Pd(II) adsorption.

Model	Parameter	COP-1	COP-2
Langmuir	q_m (mg/g)	258	318
	b_l (L/mg)	0.0751	0.0601
	R^2	0.997	0.998
Freundlich	n	3.78	3.89
	K_F (mg^{1-n} $L^{1/n}$ g^{-1})	53.1	68.7
	R^2	0.797	0.963

Table S2 Comparison of Pd adsorption capacity of COPs with other materials in HNO_3 solution (T=298 K).

Sorbents	Acidity (M HNO_3)	Capacity (mg/g)	Ref.
MXene-45	0.1	185	7
Fe_3O_4@SiO_2@DOTA	1	11	8
TpPa-1/SiO_2-A600	1	13	9
SBA-15-Cyclen	1	77	10
ACGSi	1	163	11
COF-TzDa	1	265	12
TEHTDGA	2	38	13
AP-XAD16	3	8	14
ACAM-XAD16	3	9	15
Tulsion CH-95	3	20	16
ASUiO-66	3	4	17
KNiHC/SiO_2	3	46	18
isoBu-BTP/SiO_2-P	3	69	19
Me_2-CA-BTP/SiO_2-P	3	85	20
Im-NO_3	3	88	21
CTF-S	3	333	22
CPTPN-NO_3	3	390	23
COP-1	3	258	This work
COP-2	3	318	This work

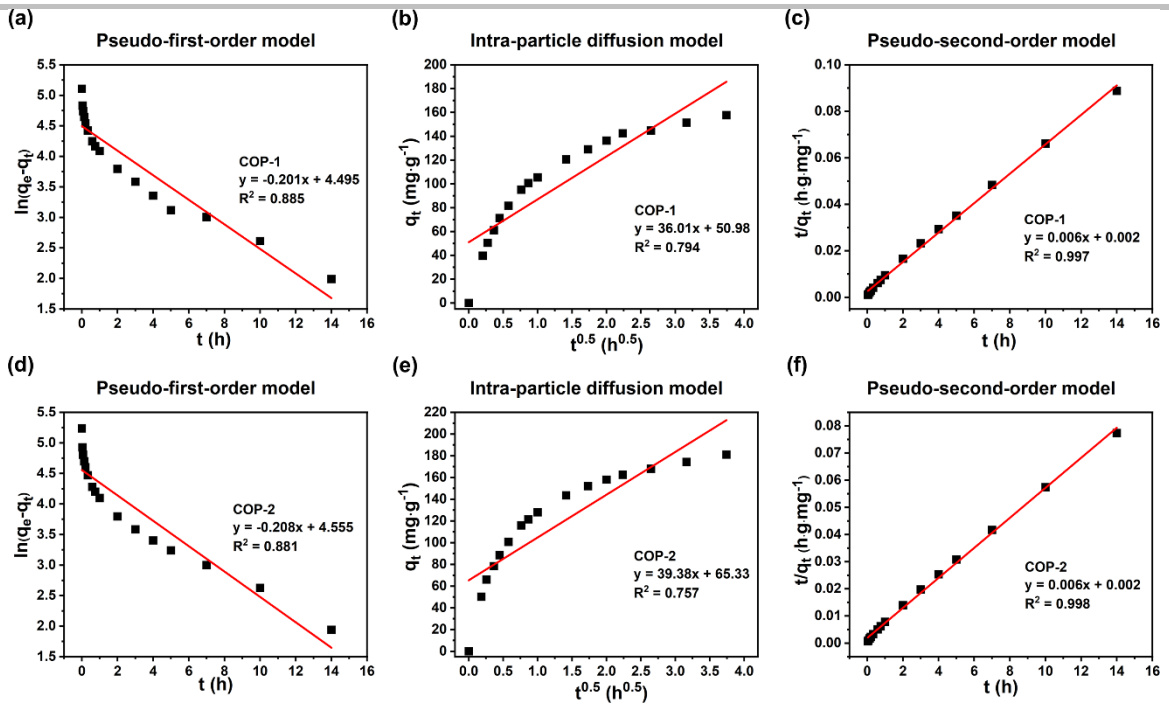

Fig. S9 (a) Pseudo-first-order, (b) pseudo-second-order, and (c) intra-particle diffusion plots for the palladium sorption onto COP-1, (d) Pseudo-first-order, (e) pseudo-second-order, and (f) intra-particle diffusion plots for the palladium sorption onto COP-2.

Table S3 Adsorption kinetics parameters for Pd(II) adsorption.

Adsorption kinetics models	Parameter	COP-1	COP-2
Pseudo-first-order model	q_e (mg g^{-1})	90	95
	k_1 (h^{-1})	0.201	0.208
	R^2	0.885	0.881
Pseudo-second-order model	q_e (mg g^{-1})	158	181
	k_2 (h^{-1})	0.0160	0.0163
	R^2	0.997	0.998
Intraparticle diffusion model	k_{int} (mg g^{-1} h$^{-0.5}$)	36.0	39.4
	C (mg g^{-1})	51.0	65.3
	R^2	0.794	0.757

Table S4 Thermodynamics parameters for Pd(II) adsorption.

	Temperature (K)	ΔH (kJ mol^{-1})	ΔS (J mol^{-1} K^{-1})	ΔG (kJ mol^{-1})
COP-1	298	15.98	59.11	-1.63
	303			-1.93
	308			-2.22
	313			-2.53
	318			-2.82
COP-2	298	41.85	150.73	-3.07
	303			-3.82
	308			-4.57
	313			-5.33
	318			-6.08

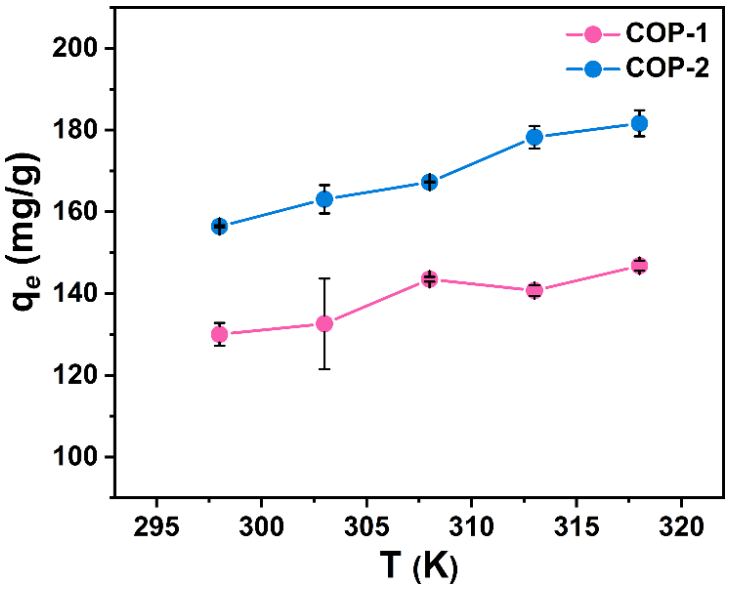

Fig. S10 Effect of temperature on the Pd(II) adsorption by COP-1 and COP-2.

Table S5 Data for the Pd(II) adsorption of COP-1 and COP-2 in simulated HLLW solution (3 M HNO_3).

Metal ion	C_0 (mg L^{-1})	COP-1			COP-2		
		C_e (mg L^{-1})	K_d (mL g^{-1})	$SF_{Pd/M}$	C_e (mg L^{-1})	K_d (mL g^{-1})	$SF_{Pd/M}$
Pd(II)	92	13	12058		4	44818	
Ni(II)	70	70	---	$>1.7 \times 10^3$	70	---	$>5.0 \times 10^3$
La(III)	275	274	12	1.0×10^3	272	20	2.2×10^3
Cd(II)	27	27	25	4.8×10^2	27	9	5.0×10^3
Eu(III)	42	42	---	$>1.7 \times 10^3$	42	---	$>5.0 \times 10^3$
Yb(III)	95	95	---	$>1.7 \times 10^3$	95	---	$>5.0 \times 10^3$
Sm(III)	136	136	---	$>1.7 \times 10^3$	137	---	$>5.0 \times 10^3$
Pr(III)	131	132	---	$>1.7 \times 10^3$	132	---	$>5.0 \times 10^3$
Ba(II)	282	282	---	$>1.7 \times 10^3$	282	---	$>5.0 \times 10^3$
Sr(II)	197	199	---	$>1.7 \times 10^3$	201	---	$>5.0 \times 10^3$
Fe(III)	218	219	---	$>1.7 \times 10^3$	218.	---	$>5.0 \times 10^3$
Nd(III)	415	412	16	7.3×10^2	411	22	2.1×10^3
Rb(I)	125	124	7	1.7×10^3	122	40	1.1×10^3
Cs(I)	670	648	68	1.8×10^2	648	66	6.8×10^2
Ag(I)	7	3	2362	5	6	363	1.2×10^2
Re(VII)	182	183	---	$>1.7 \times 10^3$	183	---	$>5.0 \times 10^3$
Mo(VI)	602	600	---	$>1.7 \times 10^3$	600	---	$>5.0 \times 10^3$
Na(I)	1111	1113	---	$>1.7 \times 10^3$	1115	---	$>5.0 \times 10^3$

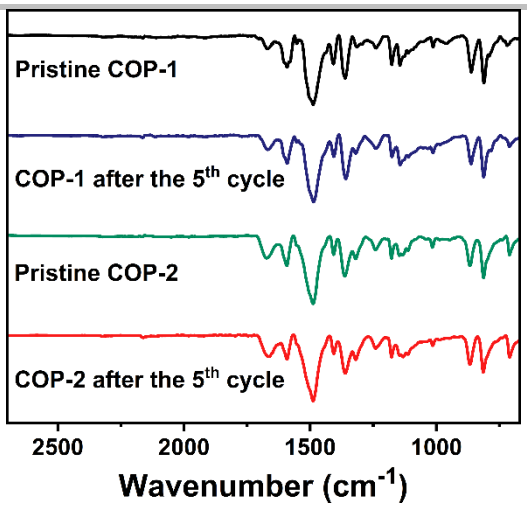

Fig. S11 FT-IR spectra of COP-1, COP-2 and the COPs used for 5 adsorption-desorption cycles.

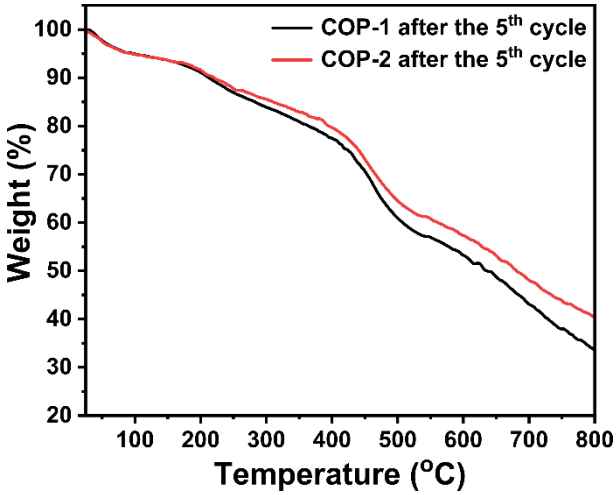

Fig. S12 TGA curves of COP-1 and COP-2 after 5 cycles.

5. Adsorption Mechanism

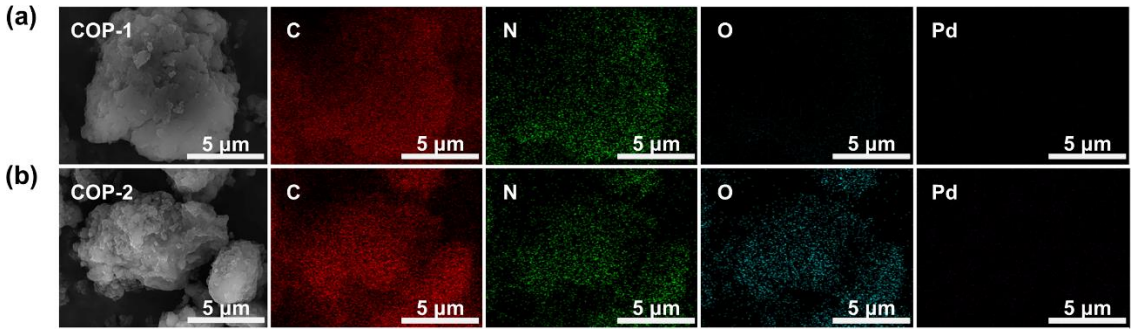

Fig. S13 SEM and EDS mapping images of (a) COP-1 and (b) COP-2.

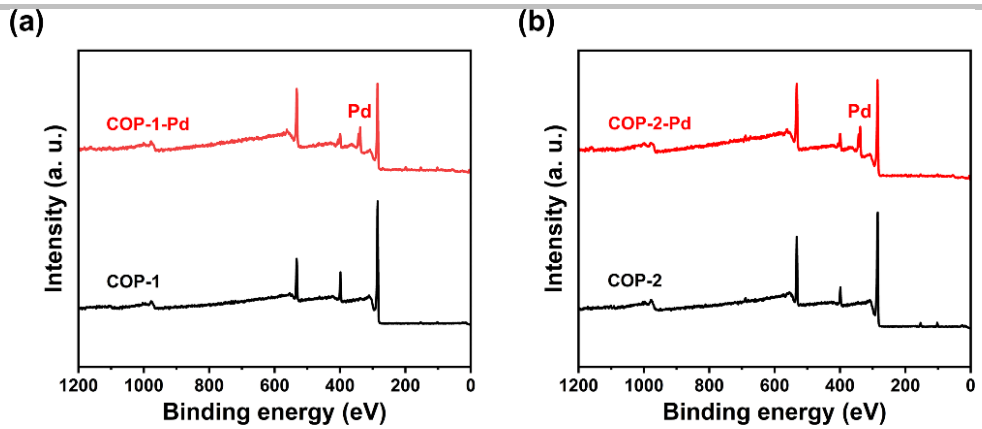

Fig. S14 Full XPS spectra of (a) COP-1 and (b) COP-2.

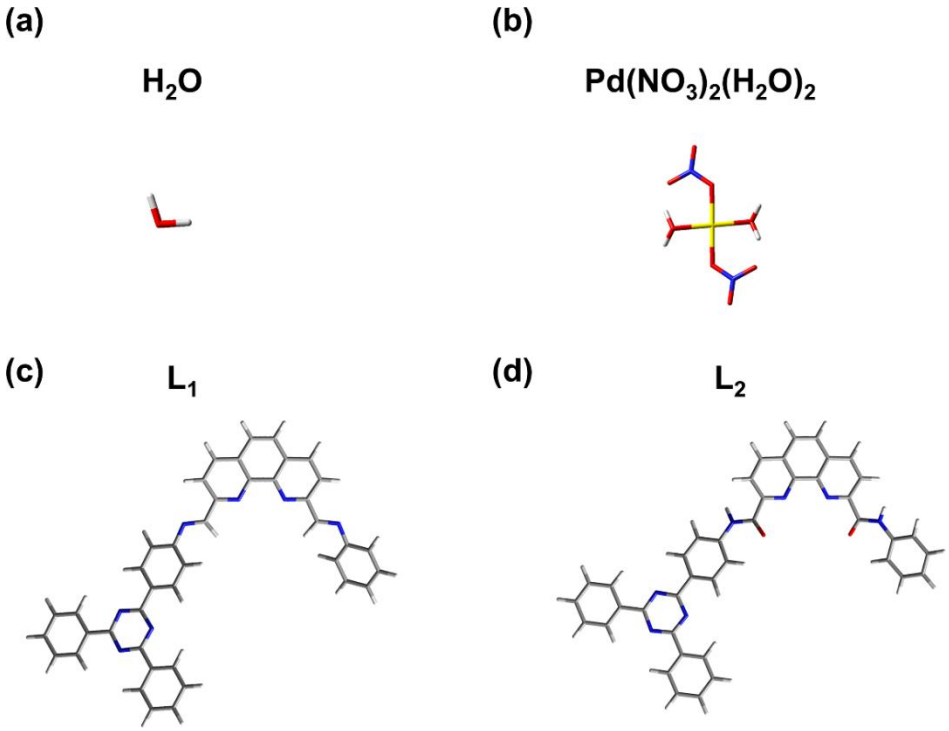

Fig. S15 Optimized geometries of the configuration corresponding to the (a) H_2O, (b) $Pd(NO_3)_2(H_2O)_2$, (c) **L1,** and (d) **L2**.

6. Catalytic Activity of COP-2-Pd(II)

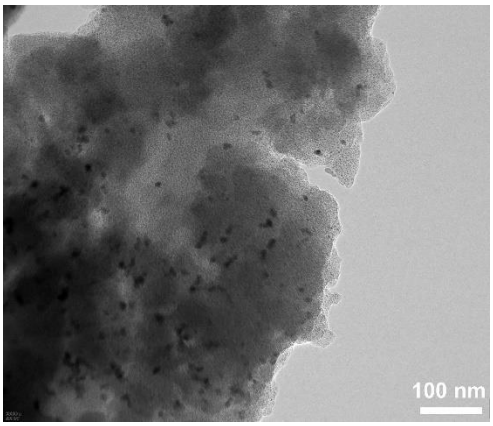

Fig. S16 TEM image of COP-2-Pd(0).

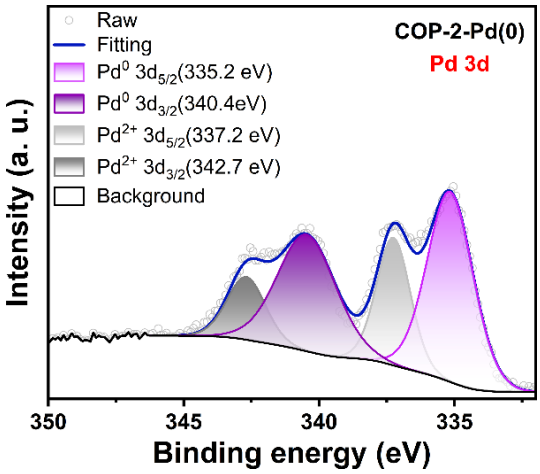

Fig. S17 Pd 3d spectra of COP-2-Pd(0).

Table S6 Elemental analysis of the spent COP-2-Pd(II).

% Calculated				% Experimental			
C	H	O	N	C	H	O	N
48	2.4	18.3	16	49	3	14	11

Table S7 The catalytic performance of COP-2-Pd(II) and previously reported Pd-based catalysts for the coupling reaction of bromobenzene and phenylboronic acid.

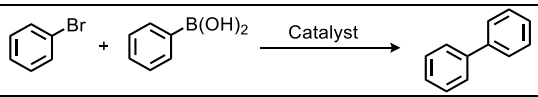

Entry	Catalyst	Solvents	Base	Temp (°C)	Mol% of Catalyst	Time (h)	Yield (%)	Recycle	TON	TOF (h^{-1})	Ref.

1	PCN-160-Pd	Toluene	K_2CO_3	90	2	12	96	4	48	4	24
2	Pd/COF-LZU1	p-xylene	K_2CO_3	150	0.5	3	97	4	194	65	25
3	UiO-66-Pyta-Pd	EtOH	K_2CO_3	80	---	2	80	3	---	---	26
4	$Pd(NH_3)_4Cl_2$	H_2O/Triton X-100	TBAOH	45	0.56	2	>99	8	178	89	27
5	Pd@CITCF-500	DMF/H_2O	Na_2CO_3	100	17.4	16	78	5	5	0.3	28
6	mPAN-Pd	H_2O	K_2CO_3	80	2	14	81	5	40	3	29
7	catalyst	H_2O	K_2CO_3	60	0.08	10	97	9	1212	121	30
8	SiO_2–*p*A–Cyan–Cys–Pd	H_2O	K_2CO_3	100	0.5	5.5	88	5	176	32	31
9	$Pd(OAc)_2/L_1$	H_2O	K_2CO_3	90	0.5	2	86	---	172	86	32
10	Mag-IL-Pd	H_2O	K_2CO_3	60	0.025	7.5	82	10	3280	437	33
11	C8NG/$Pd(OAc)_2$	H_2O	K_2CO_3	25	2	0.67	92	5	46	69	34
12	PPI-2-NPy-Pd	H_2O	$(i\text{-}Pr)_2NH$	100	0.5	0.5	>99	7	200	580	35
13	Pd@COF-QA	H_2O	TEA	50	1.7	6	99	10	58	10	36
14	Pd/TATAE	H_2O	K_2CO_3	25	0.052	2	98	4	1889	944	37
15	Pd@COF-NHC	H_2O	K_2CO_3	25	0.5	1	99	8	198	198	38
16	COP-2-Pd(II)	H_2O	K_2CO_3	100	1	5	95	20	95	19	This work

7. References

[1] I. Langmuir, *J. Am. Chem. Soc.*, 1916, **38**, 2221.

[2] H. Freundlich, *Z Phys Chem (N F)*, 1907, **57U**, 385.

[3] S. Ahn, D. Werner, H. K. Karapanagioti, D. R. McGlothlin, R. N. Zare and R. G. Luthy, *Environ. Sci. Technol.*, 2005, **39**, 6516-6526.

[4] J. Li, X. Dai, L. Zhu, C. Xu, D. Zhang, M. A. Silver, P. Li, L. Chen, Y. Li, D. Zuo, H. Zhang, C. Xiao, J. Chen, J. Diwu, O. K. Farha, T. E. Albrecht-Schmitt, Z. Chai and S. Wang, *Nat. Commun.*, 2018, **9**, 3007.

[5] R. Gomes, P. Bhanja, A. Bhaumik, *Chem. Commun.*, 2015, **51**, 10050.

[6] N. T. Coogan, M. A. Chimes, J. Raftery, P. Mocilac, M. A. Denecke, *J. Org. Chem.*, 2015, **80**, 8684.

[7] W. Mu, S. Du, X. Li, Q. Yu, H. Wei, Y. Yang, S. Peng, *Chem. Eng. J.*, 2019, **358**, 283.

[8] F. Wu, G. Ye, R. Yi, T. Sun, C. Xu, J. Chen, *Dalton Trans.*, 2016, ***45***, 9553.

[9] H. Wu, T. Kudo, T. Takahashi, T. Ito, S.-Y. Kim, *J. Radioanal. Nucl. Chem.*, 2021, **330**, 1065.

[10] F. Wu, G. Ye, Y. Liu, R. Yi, X. Huo, Y. Lu, J. Chen, *RSC Adv.*, 2016, **6**, 66537.

[11] Y. Leng, J. Xu, J. Wei, G. Ye, *Chem. Eng. J.*, 2013, **232**, 319.

[12] Y. Bai, L. Chen, L. He, B. Li, L. Chen, F. Wu, L. Chen, M. Zhang, Z. Liu, Z. Chai, S. Wang, *Chem*, 2022, **8**, 1442.

[13] N. Osawa, M. Kubota, H. Wu, S.-Y. Kim, *Sep. Sci. Technol., (Philadelphia, PA, U. S.)* 2021, **57**, 48.

[14] R. Ruhela, K. K. Singh, B. S. Tomar, J. N. Sharma, M. Kumar, R. C. Hubli, A. K. Suri, *Sep. Purif. Technol.*, 2012, **99**, 36.

[15] R. Ruhela, K. Singh, B. S. Tomar, T. K. Shesagiri, M. Kumar, R. C. Hubli, A. K. Suri, *Ind. Eng. Chem. Res.*, 2013, **52**, 5400.

[16] K. A. Venkatesan, B. R. Selvan, M. P. Antony, T. G. Srinivasan, P. R. Vasudeva Rao, *J. Radioanal. Nucl. Chem.*, 2005, **266**, 431.

[17] M. Zha, J. Liu, Y.-L. Wong, Z. Xu, *J. Mate. Chem. A*, 2015, **3**, 3928.

[18] Q. Wang, H. Sang, L. Chen, Y. Wu, Y. Wei, *Sep. Purif. Technol.*, 2020, **231**, 115932.

[19] Q. Zou, Y. Wu, Q. Shu, S. Ning, X. Wang, Y. Wei, F. Tang, *J. Chem. Eng. Data*, 2018, **63**, 2931.

[20] Q. Zou, R. Liu, S. Ning, X. Wang, Y. Wei, *J. Nucl. Sci. Technol.*, 2017, **54**, 569.

[21] K. A. Venkatesan, B. R. Selvan, M. P. Antony, T. G. Srinivasan, P. R. Vasudeva Rao, *Hydrometallurgy*, 2007, **86**, 221.

[22] P. Wu, H. Liu, M. Sun, Y. Zeng, J. Ye, S. Qin, Y. Cai, W. Feng, L. Yuan, *J. Mater. Chem. A*, 2021, **9**, 27320.

[23] X. Yuan, Y. Wang, P. Wu, X. Ouyang, W. Bai, Y. Wan, L. Yuan, W. Feng, *Chem. Eng. J.*, 2022, **430**, 132618.

[24] W. Chen, P. Cai, P. Elumalai, P. Zhang, L. Feng, M. m. Al-Rawashdeh, S. T. Madrahimov and H.-C. Zhou, *ACS Appl. Mater. Interfaces*, 2021, **13**, 51849-51854.

[25] S.-Y. Ding, J. Gao, Q. Wang, Y. Zhang, W.-G. Song, C.-Y. Su and W. Wang, *J. Am. Chem. Soc*, 2011, **133**, 19816-19822.

[26] S. Daliran, M. Ghazagh-Miri, A. R. Oveisi, M. Khajeh, S. Navalón, M. Âlvaro, M. Ghaffari-Moghaddam, H. Samareh Delarami and H. García, *ACS Appl. Mater. Interfaces*, 2020, **12**, 25221-25232.

[27] Y. Wang, Y. Liu, W.-q. Zhang, H. Sun, K. Zhang, Y. Jian, Q. Gu, G. Zhang, J. Li and Z. Gao, *ChemSusChem*, 2019, **12**, 5265-5273.

[28] K. S. Song, T. Ashirov, S. N. Talapaneni, A. H. Clark, A. V. Yakimov, M. Nachtegaal, C. Copéret and A. Coskun, *Chem*, 2022, **8**, 2043-2059.

[29] P. R. Sruthi, R. Roopak and S. Anas, *ChemistrySelect*, 2023, **8**, e202204374.

[30] M. Gholinejad, F. Hamed and P. Biji, *Dalton Trans.*, 2015, **44**, 14293-14303.

[31] M. Ghiaci, M. Zarghani, F. Moeinpour and A. Khojastehnezhad, *Appl. Organomet. Chem.*, 2014, **28**, 589-594.

[32] M. Amini, A. Tarassoli, S. Yousefi, S. Delsouz-Hafshejani, M. Bigdeli and M. Salehifar, *Chin. Chem. Lett.*, 2014, **25**, 166-168.

[33] B. Karimi, F. Mansouri and H. Vali, *Green Chem.*, 2014, **16**, 2587-2596.

[34] S. Wu, S. Zhang, X. Yang, X. Liu and X. Ge, *ACS Appl. Nano Mater.*, 2023, **6**, 1592-1602.

[35] E. Rangel Rangel, E. M. Maya, F. Sánchez, J. G. de la Campa and M. Iglesias, *Green Chem.*, 2015, **17**, 466-473.

[36] J.-C. Wang, C.-X. Liu, X. Kan, X.-W. Wu, J.-L. Kan and Y.-B. Dong, *Green Chem.*, 2020, **22**, 1150-1155.

[37] V. Sadhasivam, R. Balasaravanan, C. Chithiraikumar and A. Siva, *ChemistrySelect*, 2017, **2**, 1063-1070.

[38] J. Yang, Y. Wu, X. Wu, W. Liu, Y. Wang and J. Wang, *Green Chem.*, 2019, **21**, 5267-5273.